J. Fluid Mech. (1979), *vol.* 91, *part* 3, *pp.* 581–597
Printed in Great Britain

A numerical comparison of velocity-based and strain-based Lagrangian-history turbulence approximations

By JACKSON R. HERRING

Advanced Study Program, National Center for Atmospheric Research, Boulder, Colorado 80307

AND ROBERT H. KRAICHNAN

Dublin, New Hampshire 03444

(Received 23 May 1978)

The abridged Langrangian-history direct-interaction (ALHDI) approximation (Kraichnan 1966) and the strain-based abridged Lagrangian-history direct-interaction (SBALHDI) approximation (Kraichnan & Herring 1978) are integrated numerically for isotropic turbulence in two and three dimensions and compared with data. At moderate Reynolds numbers in three dimensions, comparison with the computer simulations by Orszag & Patterson (1972) shows that the ALHDI gives numerically excessive energy transfer in the dissipation range while the SBALHDI approximation displays satisfactory accuracy in all ranges. In two dimensions, both approximations are in reasonable agreement with the simulations of Herring *et al.* (1974), the ALHDI approximation showing the better accuracy of the two at low wavenumbers. At high wavenumbers the SBALHDI approximation again transfers less energy than the ALHDI approximation but the effect is less marked than in three dimensions and the two curves straddle the data. High Reynolds number integrations of both approximations in three dimensions agree well with the tidal-channel inertial- and dissipation-range data of Grant, Stewart & Moilliet (1962), the SBALHDI approximation yielding a somewhat larger value of Kolmogorov's constant than the ALHDI approximation. The origin of the difference in straining efficiency between the two approximations at high wavenumbers and of the dependence of this difference on dimensionality is exhibited by application to the stretching of small scales of a convected passive scalar field. In three dimensions the SBALHDI approximation gives markedly larger values of the constant in Batchelor's (1959) k^{-1} spectrum range than the ALHDI approximation and is in better agreement with experiment. The SBALHDI values of Batchelor's constant satisfy Gibson's (1968) lower bound while the ALHDI values do not.

1. Introduction

In a recent paper (Kraichnan & Herring 1978, cited hereafter as I) we have proposed a variant of the abridged Lagrangian-history direct-interaction (ALHDI) approximation for incompressible turbulence (Kraichnan 1965, 1977). The ALHDI approximation is based on the correlation between the velocity at a given space-time point and the velocity measured at earlier times along the fluid-particle trajectory passing through that point. In the new approximation the correlations of the symmetric straining field

0022–1120/79/4208–6100 $02.00

along the particle trajectories form the fundamental basis. It is therefore called the strain-based abridged Lagrangian-history direct-interaction (SBALHDI) approximation.

The present paper describes numerical integrations of the two approximations for decaying isotropic turbulence in two and three dimensions. The results are compared with computer simulations at moderate Reynolds numbers and with the tidal-channel data of Grant *et al.* (1962) at high Reynolds number.

The Eulerian symmetric straining field is defined in terms of the Eulerian velocity field by

$$b_{ij}(\mathbf{x},t) = \partial u_i(\mathbf{x},t)/\partial \mathbf{x}_j + \partial u_j(x,t)/\partial x_i. \tag{1.1}$$

The velocity and straining field values measured at time s along the fluid-particle trajectory which passes through $(\mathbf{x},t)$ are denoted by $u_i(\mathbf{x},t|s)$ and $b_{ij}(\mathbf{x},t|s)$, respectively. The differences between the ALHDI and SBALHDI approximations arise from the fact that in general

$$b_{ij}(\mathbf{x},t|s) \neq \partial u_i(\mathbf{x},t|s)/\partial x_j + \partial u_j(\mathbf{x},t|s)/\partial x_i \tag{1.2}$$

unless $t = s$. As noted in I, (1.2) has a simple meaning. The left-hand side of (1.2) is the rate-of-strain tensor measured at time s on the trajectory, while the right-hand side is proportional to the velocity difference at time s between the trajectory passing through $(\mathbf{x},t)$ and an infinitesimally displaced trajectory passing through $(\mathbf{x}+\delta\mathbf{x},t)$. The displacement between the trajectories varies with s and in general is not $\delta\mathbf{x}$ unless $t = s$. Thus the velocity difference at time s is not simply proportional to the local Eulerian velocity gradient. The dynamical implications of (1.2) have been discussed in I and will be returned to later in interpreting the numerical results.

The underlying motivation of the SBALHDI approximation is that a theory in which straining plays the fundamental role may be more faithful in representing the straining of small scales than one in which velocity is considered fundamental. The present numerical investigation provides some tests of this idea.

2. The ALHDI and SBALHDI equations for isotropic turbulence

The ALHDI approximation for isotropic turbulence (Kraichnan 1965, 1977) yields a closed set of equations involving only the defining scalar $U(k,t|s)$ of the Lagrangian velocity correlation and a corresponding scalar $G(k,t|s)$ associated with the averaged Green's tensor for response of the velocity field to infinitesimal perturbations. $U(k,t|s)$ satisfies

$$\langle u_i(\mathbf{x},t)\, u_i(\mathbf{x}',t|s)\rangle = \int U(k,t|s) \exp\left[i\mathbf{k}.(\mathbf{x}-\mathbf{x}')\right] d\mathbf{k}. \tag{2.1}$$

The final equations for the SBALHDI approximation involve instead the defining scalar of the Lagrangian strain correlation $U^B(k,t|s)$ and a corresponding response scalar $G^B(k,t|s)$ for the straining field. Because of the relation (1.1) between Eulerian velocity and straining fields, $U^B(k,t|s)$ may be written in terms of velocity–strain correlations and satisfies

$$\langle u_i(\mathbf{x},t)\, \partial b_{in}(\mathbf{x}',t|s)/\partial x_n'\rangle = -\int k^2 U^B(k,t|s) \exp\left[i\mathbf{k}.(\mathbf{x}-\mathbf{x}')\right] d\mathbf{k}. \tag{2.2}$$

It follows from (1.1) and (1.2) that

$$U^B(k,t|t) = U(k,t|t) \tag{2.3}$$

and
$$U^B(k,t|s) \neq U(k,t|s) \quad (t \neq s). \tag{2.4}$$

If $E(k,t)$ is the energy spectrum, such that

$$\int_0^\infty E(k,t)\,dk$$

is the kinematic energy per unit mass, then

$$E(k,t) = \begin{cases} 2\pi k^2 U(k,t|t) & \text{(three dimensions),} \\ \pi k U(k,t|t) & \text{(two dimensions).} \end{cases} \tag{2.5}$$

Both the ALHDI and the SBALHDI equation sets may be written in the following form:

$$(\partial/\partial t + 2\nu k^2)\, U(k,t|t) = 2\int_\Delta dp\,dq\, C^3_{kpq} \int_{t_0}^t ds\, [G(k,t|s)\, U(p,t|s) - G(p,t|s)\, U(k,t)s)]\, U(q,t|s), \tag{2.6}$$

$$\begin{aligned}(\partial/\partial t + \nu k^2)\, U(k,t|r) &= \int_\Delta dp\,dq\, C^0_{kpq} \int_r^t U(k,t|s)\, U(q,t|r)\, ds + \int_0^\infty dp\, K_{kp}\, U(p,t|r) \\ &+ \int_\Delta dp\,dq \int_{t_0}^r [C^3_{kpq}\, G(k,r|s)\, U(p,t|s) - C^4_{kpq}\, G(p,r|s)\, U(k,t|s)]\, U(q,t|s)\, ds \\ &- \int_\Delta dp\,dq \int_{t_0}^t [C^3_{kpq}\, G(p,t|s)\, U(k,r|s) - C^2_{kpq}\, G(k,t|s)\, U(p,r|s)]\, U(q,t|s)\, ds \\ &- \int_\Delta dp\,dq \int_{t_0}^t C^7_{kpq}\, G(p,t|s)\, U(k,t|s)\, U(q,r|s)\, ds,\end{aligned} \tag{2.7}$$

$$\begin{aligned}(\partial/\partial t + \nu k^2)\, G(k,t|r) &= \int_\Delta dp\,dq\, C^0_{kpq} \int_r^t G(k,t|s)\, U(q,\, t|r)\, ds + \int_0^\infty dp\, \tilde{K}_{kp}\, G(p,t|r) \\ &- \int_\Delta dp\,dq \int_r^t [C^3_{kpq}\, G(p,t|s)\, G(k,s|r) - C^4_{kpq}\, G(k,t|s)\, G(p,s|r)]\, U(q,t|s)\, ds,\end{aligned} \tag{2.8}$$

Here K_{kp} and $\tilde{K}_{kp}$ are defined by

$$K_{kp} = \int_r^t ds \left[-\delta(k-p) \int_0^\infty dp' \int_{|k-p'|}^{k+p'} dq\, C'_{kp'q} + \int_{|k-p|}^{k+p} dq\, C^2_{kpq} \right] U(q,t|s) \tag{2.9a}$$

and

$$\tilde{K}_{kp} = K_{kp} - \int_r^t ds \int_{|k-p|}^{k+p} dq\, C^8_{kpq}\, G(k,s|r)\, U(q,t|r), \tag{2.9b}$$

ν is kinematic viscosity and $\int_\Delta$ denotes integration over all p and q which can form a triangle with k. The velocity field is assumed to be normally distributed at the initial time t_0.

In the case of the SBALHDI equations U and G must be replaced by U^B and G^B everywhere in (2.6)–(2.9). Apart from this, the two approximations differ only in the coefficients C, whose form as functions of k, p, and q are given in the appendix. For derivations of (2.6)–(2.9) we refer to Kraichnan (1965, 1977) and I. We have written these equations here in a form convenient for numerical work.

The numerical integration methods used here to treat (2.6)–(2.8) have been partially described in Herring & Kraichnan (1971). Discretization of the wavenumber domain is effected by cubic splines. Let k_n ($n = 1, 2, \ldots, N$) be a set of wavenumber points at

Run	Dimensions	$E(0)$	$\epsilon(0)$	$k_{\min}$	$k_{\max}$	l†	R_l†	dt	ν	N
1	3	1·5	0·85	1·00	31·1	0·42	42·0	0·025 (DI) 0·04 (ALHDI)	0·01	20
2	3	1·5	3·63	1·00	31·1	0·20	19·7	0·025 (DI) 0·04 (ALHDI)	0·001	20
3	2	1·5	—	1·00	63·0	0·90	58·6	0·04	0·005	20
4	2	1·3	0·10	1·00	63·0	0·685	308·0	0·04	0·0025	20
5	3	37·1	19·3	0·125	64·0	—	244·0	0·02	0·008	20

† For runs 1, 2 and 5, l and R_l are the Taylor microscale and corresponding Reynolds number, while for the two-dimensional runs 3 and 4 these are the enstrophy-based integral scale and Reynolds number, as defined by Lilly [see Herring *et al.* 1974, equations (2.9) and 2.10)].

TABLE 1

which the integration on the right-hand side of (2.6)–(2.8) is to be performed. Then we approximate $U(k)$ and $G(k)$ by

$$U(k) = \sum_{n=1}^{N} U(k_n)\,\phi_n(k), \quad \phi_n(k_m) = \delta_{nm},$$

$$G(k) = \sum_{1}^{N} G(k_n)\,\phi_n(k),$$

and compute (and store) the integrals of the B_{kpq} and C_{kpq} functions over appropriate products of cardinal functions $\phi_n(p)$ and $\phi_m(q)$, thereby replacing the $dp\,dq$ integrals in (2.6)–(2.8) by finite sums. In practice, these numerical integrations are effected by Gaussian methods, and the integrals over $\phi_n(p)$ and $\phi_m(q)$ are replaced by equivalent, but more economical, ones over B-splines (de Boor 1977).

Our treatment of the time integration is somewhat different from that which we have used before. The most important new element is to regard the quasi-linear terms νk^2, $K(k,p)$ and $\tilde{K}(k,p)$ in (2.7) and (2.8) as specified during a time step, and the remaining terms in these equations as a forcing function for $\partial U(k,t|r)/\partial t$ and $\partial G(k,t|r)/\partial t$. The effect of the quasi-linear terms is then treated exactly by using the eigenvalue and eigenfunctions generated by the operators

$$-\nu k^2\delta(k,k') + \tilde{K}(k,k'), \quad -\nu k^2\delta(k,k') + K(k,k')$$

and their adjoints. The resulting system is then written as a generalized modified Euler scheme of second order and iterated twice. This refinement is necessary to assure good convergence to the three-dimensional problem for cases in which the initial energy spectrum has little energy at large wavenumbers. In practice, invoking the needed eigenvalue routines added little to the computation time, and permitted larger time steps to be taken. The wavenumber truncation procedure used is systematically to discard any contributions to the right-hand side of (2.6)–(2.8) for which any k, p or q is outside $(k_{\min}, k_{\max})$.

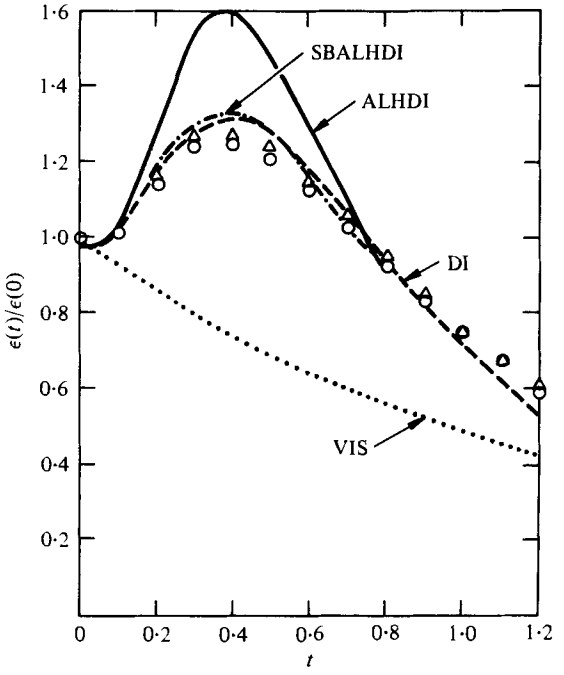

FIGURE 1. Total energy dissipation $\epsilon(t)$ according to various approximations: ——, ALHDI; ——·——, SBALHDI; – – –, DI. Initial energy spectrum is (3.1); other data for run are given in table 1. Circles and triangles show two realizations of simulations by Orszag & Patterson (1972). The dotted line gives pure viscous decay.

3. Numerical results

3.1. *Low Reynolds number in three dimensions*

We shall now compare numerical integrations of the SBALHDI and ALHDI equations with the parent direct-interaction (DI) approximation (Herring & Kraichnan 1971) and with the computer simulations of isotropic turbulence by Orszag & Patterson (1972). We consider two forms of initial energy spectra:

$$E(k, 0) = 16(2/\pi)^{\frac{1}{2}} v_0^2 k_0^{-5} k^4 \exp\left[-2(k/k_0)^2\right] \tag{3.1}$$

and

$$E(k, 0) = (\tfrac{3}{2} v_0^2 \lambda^2 k) \exp(-\lambda k). \tag{3.2}$$

We call (3.1) run 1 and (3.2) run 2. For run 1, $v_0 = 1$ and $k_0 = 4{\cdot}757$, and for run 2, $v_0 = 1$ and $\lambda = 0{\cdot}12022$. Run 1 is chosen for comparison with the Orszag–Patterson (1972) data. Run 2 evolves quickly into a self-similar spectrum of the sort found in wind-tunnel experiments. Other information needed to specify the numerical calculation (viscosity ν, cut-off wavenumbers $k_{\min}$, $k_{\max}$, length scale l, Reynolds number R_l, total energy $E(0)$, energy dissipation $\epsilon(0)$, time step dt and number of interpolation knots N) is listed in table 1. (Runs 3 and 4 listed there are similar runs for two-dimensional turbulence, and run 5 is at large Reynolds number, in three dimensions. These will be described soon.)

Figure 1 shows $\epsilon(t)$ for run 1 according to the ALHDI, SBALHDI and DI approximations and two numerical simulations of Orszag & Patterson (1972). The dotted line

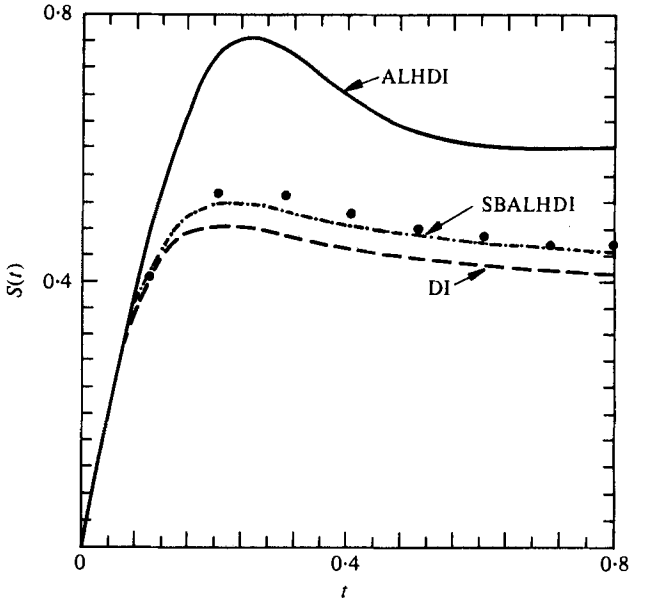

FIGURE 2. Skewness factor $S(t)$ as defined by (3.3) according to various approximations and numerical simulations for run 1. ——, ALHDI; –·–, SBALHDI; – – –, DI. Initial energy spectrum and other data same as for figure 1.

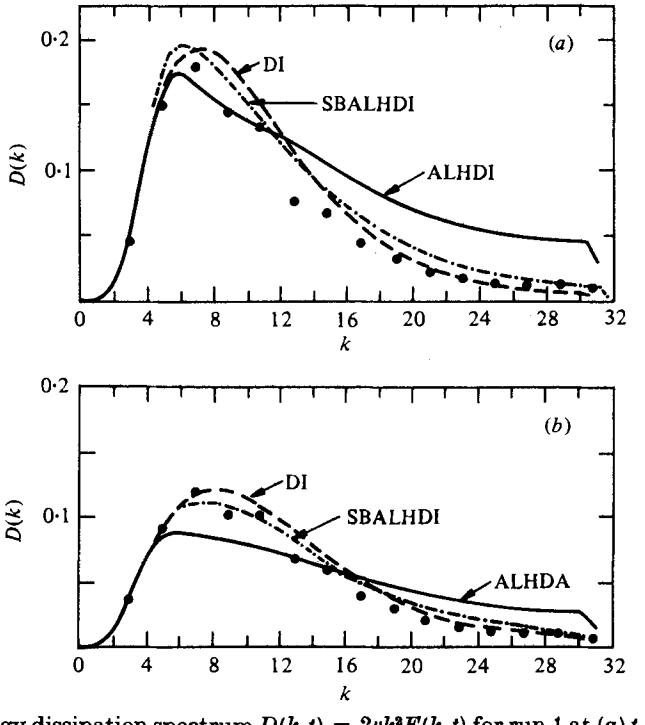

FIGURE 3. Energy dissipation spectrum $D(k,t) = 2\nu k^2 E(k,t)$ for run 1 at (*a*) $t = 0{\cdot}4$ and (*b*) $t = 0{\cdot}8$ according to various approximations and a realization of the numerical simulation ——, ALHDI; —·—, SBALHDI; – – –, DI. Initial energy spectrum and other data same as for figure 1.

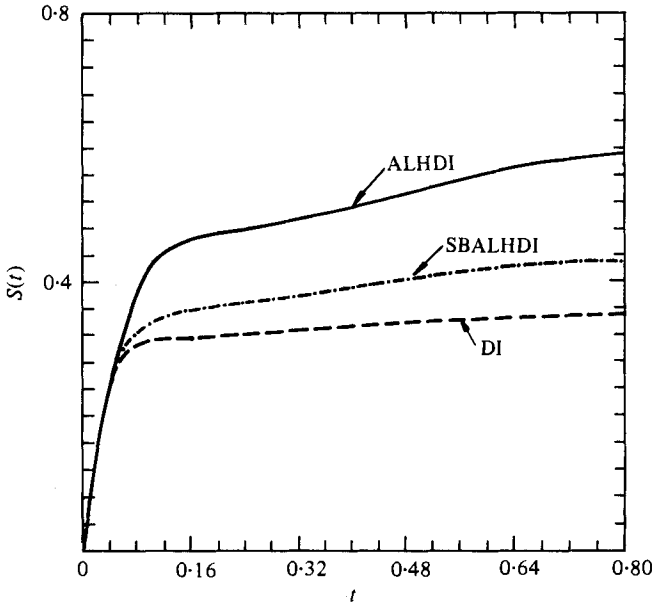

FIGURE 4. Skewness factor $S(t)$ for run 2.

here gives $\epsilon(t)$ for pure viscous decay. We notice that the DI and SBALHDI approximations and the numerical simulations are in good agreement, while the ALHDI approximation significantly overestimates the energy dissipation during the early phase. Related behaviour is displayed in figure 2 by the skewness $S(t)$, defined as

$$S(t) = \langle(\partial u_1(\mathbf{x},t)/\partial x_1)^3\rangle / \langle(\partial u_1(\mathbf{x},t)/\partial x_1)^2\rangle^{\frac{3}{2}}$$
$$= (\tfrac{35}{2})^{\frac{1}{2}} \left(\int_0^\infty k^2\,dk\,T(k,t)\right) \Big/ \left(\int_0^\infty k^2\,dk\,E(k,t)\right)^{-\frac{3}{2}}. \tag{3.3}$$

In (3.3), $T(k,t)$ is the energy transfer function, defined such that the energy spectrum satisfies

$$\partial E(k,t)/\partial t + 2\nu k^2 E(k,t) = T(k,t). \tag{3.4}$$

Again the DI and SBALHDI approximations agree well with the simulations, but for the ALHDI approximation $S(t)$ is significantly larger than the simulation value.

Figures 3(*a*) and (*b*) show the energy dissipation spectrum $D(k,t) \equiv 2\nu k^2 E(k,t)$ at $t = 0{\cdot}4$ and $0{\cdot}8$ as a function of k for run 1. At the largest wavenumbers, $D(k,t)$ for the ALHDI approximation is too large by a factor of 4 at $t = 0{\cdot}4$ and by a factor ~ 2 at $t = 0{\cdot}8$. At both times the DI approximation is in good agreement with the numerical simulations, while the SBALHDI approximation is significantly better than the ALHDI approximation but perhaps not as good as the DI approximation. The peculiar shape of the ALHDI curves for k just beyond the maximum of $D(k)$ appears to be related to the strong effect of truncating k at $k = 31$.

We have noted in § 5 of I that the ALHDI equations yield the inviscid energy-equipartition equilibrium spectra (for a system truncated in wavenumber), but that this is not true of the SBALHDI approximation. However (see I), the SBALHDI equations yield the equilibrium spectra if subjected to a slight change: the replacement

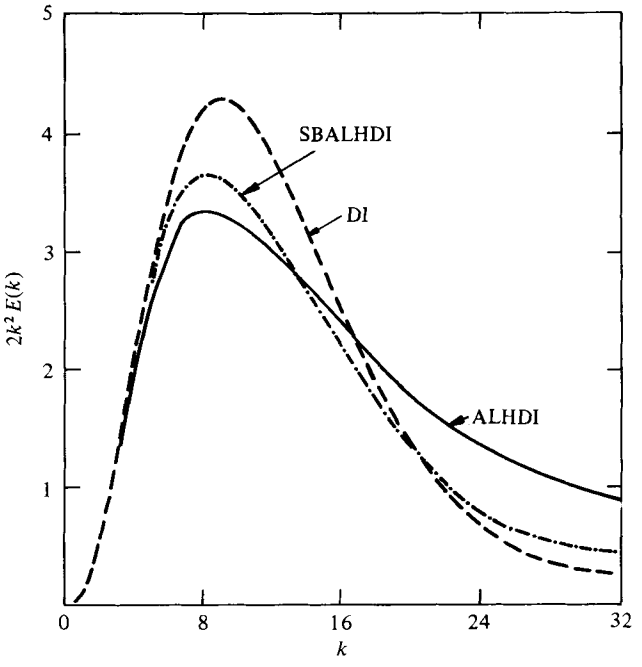

FIGURE 5. Energy dissipation spectrum $D(k, t)$ for run 2 at $t = 0{\cdot}6$.

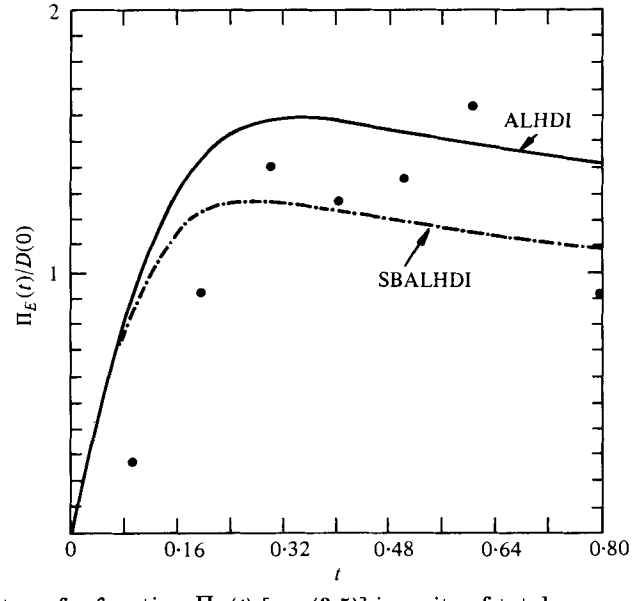

FIGURE 6. Back transfer function $\Pi_E(t)$ [see (3.5)] in units of total energy dissipation for two-dimensional run 3 (see table 1). ——, ALHDI; –·–, SBALHDI; ●, numerical simulation by Fox & Orszag (1973).

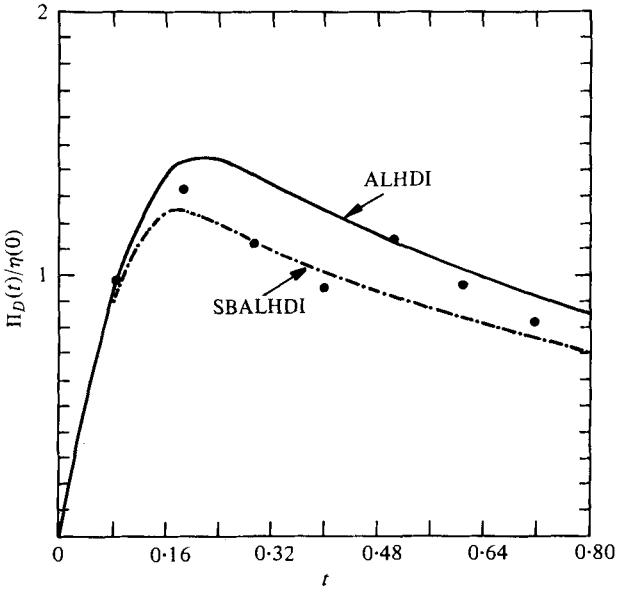

FIGURE 7. Enstrophy transfer function $\Pi_D(t)$ [see (3.6)] in units of enstrophy dissipation for two-dimensional run 4 (see table 1). ——, ALHDI; — · —, SBALHDI; ●, numerical simulation by Fox & Orszag (1973).

of C^8_{kpq} (see equation (A 8) of the appendix) by an altered coefficient in which

$$\mathbf{P}''(-q) \to \mathbf{P}(-q).$$

If this is done, the agreement with the present numerical simulation is negligibly altered; for example, for run 1 the skewness at $t = 0{\cdot}8$ is reduced from 0·4475 to 0·4442.

Figures 4 and 5 show results for the more self-similarly evolving spectrum (3.2). Figure 4 shows that the ALHDI value of the skewness exceeds the DI value by an amount roughly the same as for spectrum (3.1), whereas the SBALHDI curve is closer to the DI curve. Similarly the ALHDI dissipation spectrum (figure 5) exceeds the DI spectrum at large k by about a factor of 2, as found for run 1. We should remark that the spectral shapes for all theories become self-similar for $t > 0{\cdot}3$. Numerical simulations for the spectral shape (3.2) have yet to be done with sufficient accuracy to make comparisons with theory.

3.2. *Two dimensions*

We next examine two-dimensional turbulence, comparing the approximations with the numerical simulations by Herring *et al.* (1974). The initial spectra investigated are (3.1) (with $v_0 = 1, k_0 = 8$) and (3.2) (with $v_0 = 1$, $\lambda = \frac{2}{3}$), with other parameters of the calculation as listed in table 1. Note that the Reynolds number for run 4 is much larger than that for the previous three-dimensional run. We do not compare DI results with the simulations; previous calculations (Herring *et al.* 1974) indicated that this approximation performs poorly in the enstrophy transfer range of two-dimensional flow because it does not preserve invariance to random Galilean transformations.

Figures 6 and 7 summarize the gross energy and enstrophy transfer characteristics for run 4. Figure 6 gives the integrated energy transfer to low wavenumbers and figure

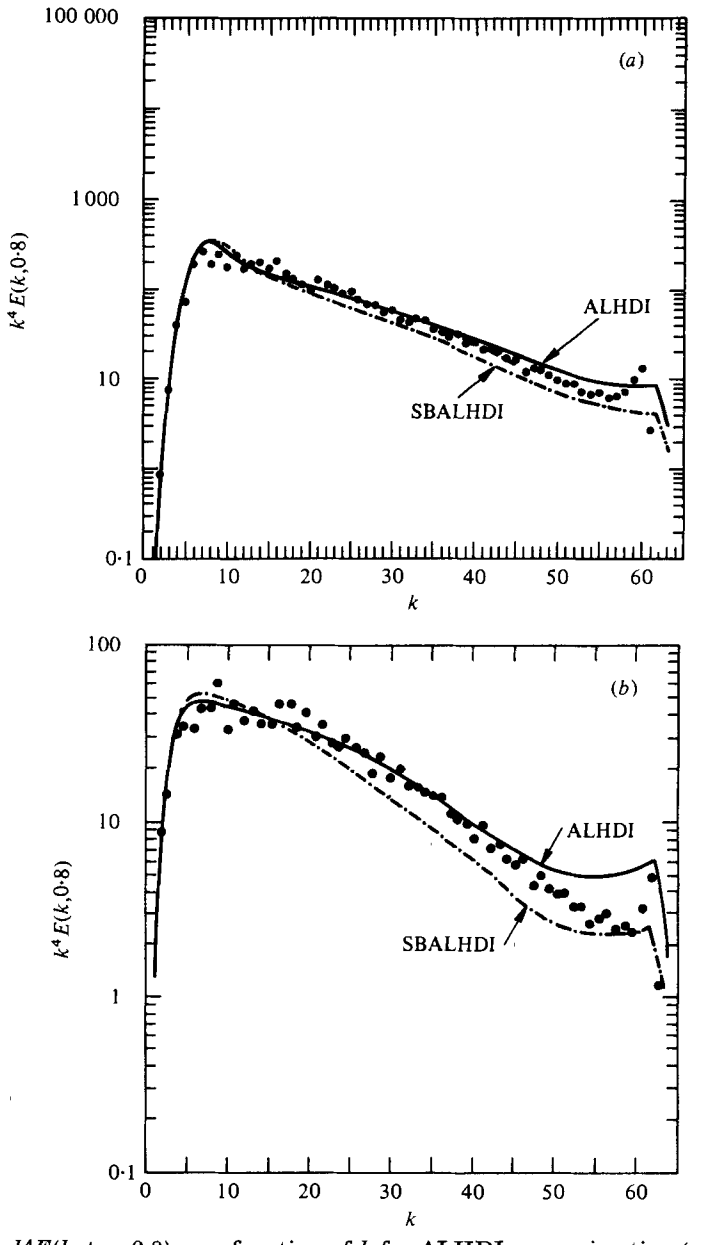

FIGURE 8. $k^4E(k, t = 0{\cdot}8)$ as a function of k for ALHDI approximation (solid line), SBALHDI approximation (dot–dash line) and Fox–Orszag simulation (points) for (*a*) run 3 and (*b*) run 4 (see table 1).

7 gives the enstrophy transfer to high wavenumbers. The first of these quantities is defined as

$$\Pi_E(t) = \int_0^{k_1} dk\, T(k,t) \tag{3.5}$$

and the latter by

$$\Pi_D(t) = \int_{k_1}^{\infty} k^2 dk\, T(k,t), \tag{3.6}$$

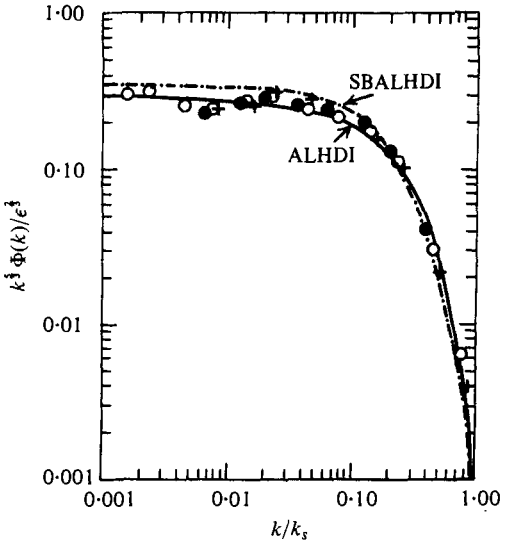

FIGURE 9. $k^{\frac{5}{3}}\phi(k)/\epsilon^{\frac{2}{3}}$ at $t = 0{\cdot}3$ as a function of k/k_s for $E(k, 0)$ given by (3.7). Here $\phi(k)$ is given by (3.8), ϵ is the dissipation of kinetic energy and k_s is the Kolmogorov wave number. Parameters are those of run 5 listed in table 1. ——, ALHDI; —·—, SBALHDI; points, data of Grant *et al.* (1962), cf. Kraichnan (1966).

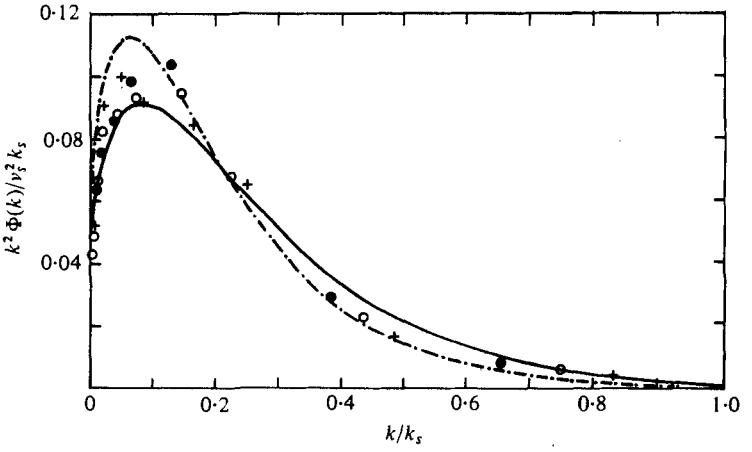

FIGURE 10. $k^2\phi(k)/v_s^2 k_s$ as a function of k/k_s at $t = 0{\cdot}2$ for $E(k, 0)$ as given by (3.7) (run 5, table 1). Here v_s and k_s are the Kolmogorov velocity and wavenumbers, and ϕ is given by (3.8). ——, ALHDI; —·—, SBALHDI; points, data of Grant *et al.* (1962).

with $T(k, t)$ as given by (3.4). Here k_1 is the smaller zero-crossing wavenumber of $T(k, t)$ and k_2 is the larger zero-crossing wavenumber. The ALHDI and SBALHDI approximations are both in reasonable agreement with the numerical simulations. We note that for two dimensions, as found previously in three dimensions, the SBALHDI approximation appears to yield a smaller energy and enstrophy transfer than the ALHDI approximation. A more detailed comparison is given in figures 8 (*a*)and (*b*), which depict the spectrum $k^4E(k, t)$ at $t = 0{\cdot}8$ for runs 3 and 4 respectively. These figures, in conjunction with figures 6 and 7, indicate a larger transfer to very small and

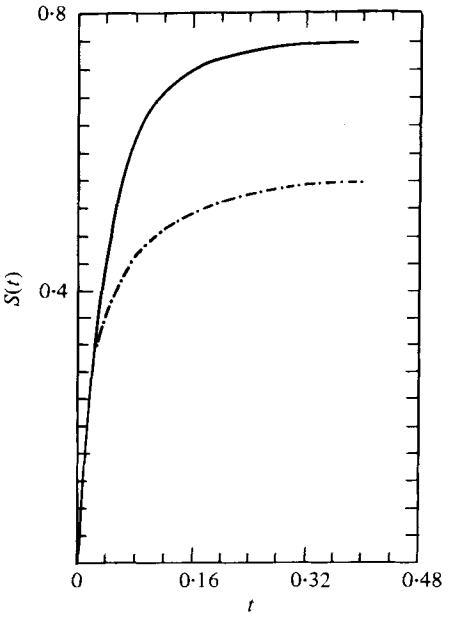

FIGURE 11. $S(t)$ as given by (3.3) for run 5 (table 1). ——, ALHDI; —·—, SBALHDI.

large wavenumbers for the ALHDI than for the SBALHDI approximation, particularly at the larger Reynolds number (run 4). The ALHDI approximation appears here to be in somewhat better agreement with simulation than the SBALHDI approximation, in contrast to the case of three dimensions at low Reynolds numbers. Overall, the agreement between the ALHDI approximation and simulations in two dimensions appears to be much more satisfactory than in three.

3.3. *Tidal-channel measurements*

In order to describe three-dimensional turbulence at large enough Reynolds numbers to approach inertial-range behaviour we take the initial spectrum as

$$E(k, 0) = 2\pi k^{-\frac{5}{3}}. \tag{3.7}$$

Other parameters for this run (run 5) are listed in table 1 and are identical to those for ALHDI calculations reported earlier (Kraichnan 1966). We have repeated these ALHDI calculations using the present numerical technique so that the role of numerical errors will be minimized in our comparison of the two theories. Our present ALHDI results are in good agreement with those reported earlier ($\sim 5\%$). Figures 9, 10 and 11 compare the approximations with the data of Grant *et al.* (1962). Figure 9 depicts the dimensionless inertial-range quantity

$$k^{\frac{5}{3}}\phi(k)/\epsilon^{\frac{2}{3}},$$

while figure 10 gives the one-dimensional dissipation function

$$k^2\phi(k)/v_s^2 k_s.$$

Here

$$\phi(k) = \frac{1}{2}\int_k^\infty \frac{dp}{p[1-(k/p)^2]}\, E(p), \tag{3.8}$$

ϵ is the dissipation of kinetic energy, k_s is the Kolmogorov wavenumber $(\nu/\epsilon^3)^{\frac{1}{4}}$ and $v_s = \nu k_s$ is the Kolmogorov velocity scale. The abscissa is k/k_s. The figures show self-similarly evolving profiles at $R_\lambda \sim 400$. This Reynolds number was found through numerical experimentation to be sufficiently large for the dissipation profiles to be asymptotic within computational error.

Both theories agree well with experiment in predicting the transition region between the inertial and dissipation ranges and in reproducing the dissipation-range data. The agreement with experiment in the far dissipation range appears to be better for the SBALHDI than for the ALHDI approximation, however this is the region where the experimental data are most uncertain. Figure 9 suggests a slightly larger Kolmogorov constant for the SBALHDI approximation ($\sim 2{\cdot}0$) compared with a value of 1·78 for the ALHDI approximation. (We have not computed a Kolmogorov constant at $R_\lambda \to \infty$ separately, as in Kraichnan 1966.) The observed trends are consistent with a slightly smaller energy transfer to large k for the SBALHDI approximation. This is also indicated by the behaviour of the skewness (3.3), which is shown in figure 11.

4. The effective straining efficiency at small scales

The preceding numerical results show stronger energy transfer at small scales in the ALHDI approximation than in the SBALHDI approximation. The effect is more marked in three dimensions than in two. In I this was predicted from properties of the Lagrangian strain covariance

$$B(t|s) = \langle b_{ij}(\mathbf{x}, t)\, b_{ij}(\mathbf{x}, t|s)\rangle = 2\int k^2 U^B(k, t|s)\, d\mathbf{k}, \tag{4.1}$$

which is related to the stretching of small-scale structures in the SBALHDI approximation, and properties of the quantity playing the analogous role in the ALHDI approximation,

$$B'(t|s) = \langle b_{ij}(\mathbf{x}, t)\, b'_{ij}(\mathbf{x}, t|s)\rangle = 2\int k^2 U(k, t|s)\, ds, \tag{4.2}$$

where $b'_{ij}(x, t|s)$ is the right-hand side of (1.2). We noted in I that $B(t|s)$ as a function of $t-s$ has zero slope if the turbulence is stationary (it is an even function of $t-s$) while the slope of $B'(t|s)$ satisfies

$$[\partial B'(t|s)/\partial t]_{t=s} = 4\int_0^\infty k^2 T(k, t)\, dk. \tag{4.3}$$

The right-hand side of (4.3) is proportional to the rate of enstrophy production. It is positive in three dimensions and zero in two dimensions. We inferred from this behaviour at $t = s$ that $B(t|s)$ should show relatively more persistence in three dimensions than in two, when compared with $B'(t|s)$. In addition to this effect, analytical results for Lagrangian statistics of a normally distributed, frozen velocity field obtained in I suggested that in both two and three dimensions $U^B(k, t|s)$ tends to have a shorter correlation time than $U(k, t|s)$ even when there is no energy transfer. Finally, (4.3) is consistent with the observation, in the integrations, of a greater difference in straining efficiency between the ALHDI and SBALHDI approximations when the initial spectrum is concentrated so that there is a strong early surge of transfer into small scales.

The relation of $B(t|s)$ and $B'(t|s)$ to the effective straining of small scales can be exhibited with particular clarity in the convection of a passive scalar field by turbulence.

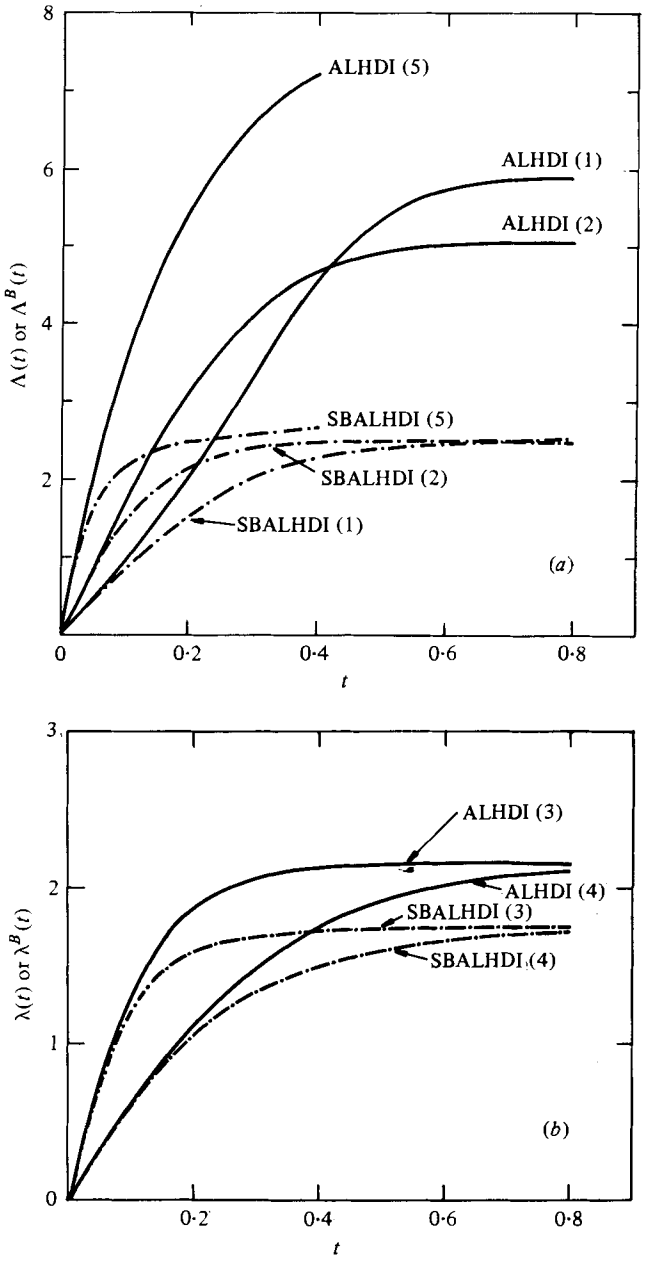

FIGURE 12. $\Lambda(t)$ and $\Lambda^B(t)$ [see (4.5) and (4.8)] as a function of t for (a) the three-dimensional runs and (b) the two-dimensional runs.

Let $F(k,t)$ be the spectrum function of an isotropically distributed passive scalar without molecular diffusivity, normalized such that

$$\int_0^\infty F(k,t)\,dk$$

is the scalar variance. If the scalar field is statistically independent of the velocity

field at $t = 0$, the ALHDI approximation for the evolution of $F(k,t)$ at values of k large compared with the wavenumbers of the velocity field gives

$$\partial F(k,t)/\partial t = [D(D+2)]^{-1}\Lambda(t)\frac{\partial}{\partial k}\left[\left(k\frac{\partial}{\partial k}-D\right)kF(k,t)\right], \tag{4.4}$$

where

$$\Lambda(t) = \frac{1}{2}\int_0^t B'(t|s)\,ds \tag{4.5}$$

and D is the dimensionality of space [cf. Kraichnan 1968, equation (4.8); 1974, equation (5.12)]. Batchelor (1959) derived for k large compared with dissipation-scale wavenumbers the spectrum

$$F(k) = C(\nu/\epsilon)^{\frac{1}{2}}\chi k^{-1}, \tag{4.6}$$

where χ is the steady rate at which scalar variance is fed into the spectrum from small wavenumbers. Equation (4.4) implies that the steady-state value of the dimensionless coefficient C is

$$C = (D+2)\,[(\nu/\epsilon)^{\frac{1}{2}}\Lambda(\infty)]^{-1} \tag{4.7}$$

[cf. Kraichnan 1974, equation (5.14)].

The right-hand side of (4.4) may be derived as the lowest order in a renormalized perturbation expansion in which moments of the velocity field are expressed in terms of the Lagrangian velocity covariance (Kraichnan 1977). If instead the moments are expressed in terms of the Lagrangian strain covariance, the lowest order yields a SBALHDI approximation for the scalar transfer function. Equations (4.4) and (4.7) are unchanged in form but $\Lambda(t)$ is replaced by

$$\Lambda^B(t) = \frac{1}{2}\int_0^t B(t|s)\,ds. \tag{4.8}$$

The numerical values of $\Lambda(t)$ and $\Lambda^B(t)$ for the several integrations of the ALHDI and SBALHDI equations are shown in figures 12(*a*) and (*b*). In accordance with the expectations stated above, the SBALHDI values for three dimensions indicate markedly less net stretching of the scalar field at small scales than the ALHDI values, while the difference is much smaller, but still present, in two dimensions.

Gibson (1968) derived bounds on the possible value of C by assuming that the straining tensor is statistically isotropic and constant in time with statistically sharp eigenvalues. For general dimensionality D his argument gives

$$[2D/(D-1)]^{\frac{1}{2}} \leqslant C \leqslant [2D(D-1)]^{\frac{1}{2}}. \tag{4.9}$$

In actual turbulence the statistical fluctuation of the eigenvalues will raise the lower bound on C (Kraichnan 1968) while the upper bound will be infinite unless the intermittency of the statistical distribution of the velocity field is bounded. Note that for $D = 2$ the two bounds for sharp eigenvalues coalesce. For both two and three dimensions the SBALHDI values of C indicated by figures 12(*a*) and (*b*) satisfy Gibson's lower bound while the ALHDI values do not. In three dimensions the SBALHDI values are reasonably consistent with the experimental measurements by Clay (1973) ($C \sim 2{\cdot}0$) while the ALHDI values are too small. There are no two-dimensional measurements.

To conclude, we mention an alternative way of applying the strain-based Lagrangian-history concept to scalar convection. The approximation just described takes the straining field and the scalar field as basic. Instead we could take the straining field

and the gradient of the scalar field as basic. This would make a difference in the final results.

We thank Mr Larry Sapp for programming assistance, particularly in implementing the B-spline scheme used in the numerical calculations. The National Center for Atmospheric Research is sponsored by the National Science Foundation. R. H. K.'s work was supported by the National Science Foundation under Grant ATM75-15100 and by the Office of Naval Research under Contracts N00014-77-C-0068 and N00014-78-C-0148.

Appendix

The coefficients entering the two- and three-dimensional ALHDI and SBALHDI approximations are built from the projection operator

$$P_{ij}(\mathbf{k}) = \delta_{ij} - k_i k_j / k^2. \tag{A 1}$$

For the SBALHDI approximation we define

$$\mathbf{P}'(\mathbf{p}) = k^{-2}[(\mathbf{k}.\mathbf{p})\mathbf{P}(\mathbf{p}) + (\mathbf{P}(\mathbf{p}).\mathbf{k})\mathbf{p}], \tag{A 2}$$

$$\mathbf{P}''(\mathbf{q}) = p^{-2}[(\mathbf{p}.\mathbf{q})\mathbf{P}(\mathbf{q}) + (\mathbf{P}(\mathbf{q}).\mathbf{p})\mathbf{q}], \tag{A 3}$$

while for the ALHDI approximation we take instead

$$P'_{ij}(\mathbf{p}) = P_{ij}(\mathbf{p}), \quad P''_{ij}(\mathbf{q}) = P_{ij}(\mathbf{q}). \tag{A 4), (A 5}$$

Then the coefficients are

$$C^0_{kpq} = \Phi_n[\mathbf{k}.\mathbf{P}'(-\mathbf{q}).\mathbf{P}(\mathbf{k}).\mathbf{q}], \tag{A 6}$$

$$C^1_{kpq} = \Phi_n[\mathbf{k}.\mathbf{P}(\mathbf{q}).\mathbf{k}]\,\mathrm{tr}\,(\mathbf{P}(\mathbf{k})), \tag{A 7}$$

$$\begin{aligned} C^3_{kpq} = \Phi_n[&\mathbf{k}.\mathbf{P}(\mathbf{p}).\mathbf{P}(\mathbf{k}).\mathbf{P}(\mathbf{q}).\mathbf{p} + \mathbf{k}.\mathbf{P}(\mathbf{p}).\mathbf{P}(\mathbf{q}).\mathbf{P}(\mathbf{k}).\mathbf{p} \\ &+ \mathbf{k}.\mathbf{P}(\mathbf{q}).\mathbf{P}(\mathbf{p}).\mathbf{P}(\mathbf{k}).\mathbf{p} + \mathbf{P}(\mathbf{k}){:}\,\mathbf{P}(\mathbf{p})\mathbf{k}.\mathbf{P}(\mathbf{q}).\mathbf{k}], \end{aligned} \tag{A 8}$$

$$C^2_{kpq} = \Phi_n[\mathbf{p}.\mathbf{P}'(\mathbf{p}).\mathbf{P}(\mathbf{k}).\mathbf{P}(\mathbf{q}).\mathbf{k} + \mathbf{P}(\mathbf{k}){:}\,\mathbf{P}'(\mathbf{p})\mathbf{k}.\mathbf{P}(\mathbf{q}).\mathbf{k}], \tag{A 9}$$

$$C^4_{kpq} = \Phi_n[\mathbf{p}.\mathbf{P}(\mathbf{q}).\mathbf{P}'(\mathbf{p}).\mathbf{P}(\mathbf{k}).\mathbf{p} + \mathbf{P}(\mathbf{k}){:}\,\mathbf{P}'(\mathbf{p})\mathbf{k}.\mathbf{P}(\mathbf{q}).\mathbf{k}], \tag{A 10}$$

$$C^7_{kpq} = \Phi_n[\mathbf{k}.\mathbf{P}(\mathbf{p}).\mathbf{P}'(\mathbf{q}).\mathbf{P}(\mathbf{k}).\mathbf{p} + \mathbf{p}.\mathbf{P}'(\mathbf{q}).\mathbf{P}(\mathbf{k}).\mathbf{P}(\mathbf{p}).\mathbf{k}], \tag{A 11}$$

$$C^8_{kpq} = \Phi_n[\mathbf{k}.\mathbf{P}''(-\mathbf{q}).\mathbf{P}(\mathbf{p}).\mathbf{P}(\mathbf{k}).\mathbf{p} + \mathbf{p}.\mathbf{P}(\mathbf{k}).\mathbf{P}''(-\mathbf{q}).\mathbf{P}(\mathbf{k}).\mathbf{k}], \tag{A 12}$$

where

$$\Phi_2 = 2/\sin(p,q) \quad \text{(for two dimensions)}, \tag{A 13}$$

$$\Phi_3 = \tfrac{1}{2}\pi pq/k \quad \text{(for three dimensions)}, \tag{A 14}$$

and $\sin(p,q)$ is the sine of the angle between p and q in the triangle formed from k, p and q. With the definitions (A 4) and (A 5), the correspondence between the ALHDI coefficients B, C, D and D' as given in Kraichnan (1966) and the present C^i is

$$(C^0, C^1, C^2, C^3, C^4, C^7, C^8) \to (0, C, D, B, D', B-D', D-B). \tag{A 15}$$

To obtain the DI equations from (2.7) and (2.8) set all coefficients except $B_{kpq} \equiv C^3_{kpq}$ as given by (A 8) equal to zero and replace all U and G functions with the corresponding Eulerian functions.

REFERENCES

BATCHELOR, G. K. 1959 Small-scale variations of convected quantities like temperature in a turbulent fluid. *J. Fluid Mech.* **5**, 113.

BOOR, C. DE 1977 Package for calculating with B-splines. *SIAM J. Numer. Anal.* **14**, 441.

CLAY, J. P. 1973 Turbulent mixing of temperature in water, air, and mercury. Ph.D. dissertation, Engng Sci. (Engng Phys.), University of California at San Diego.

FOX, D. G. & ORSZAG, S. A. 1973 Pseudospectral approximation for two-dimensional turbulence. *J. Comp. Phys.* **11**, 612.

GIBSON, C. H. 1968 Fine structure of scalar fields mixed by turbulence. II. Spectral theory. *Phys. Fluids* **11**, 2316.

GRANT, H. L., STEWART, R. W. & MOILLIET, A. M. 1962 Turbulent spectra from a tidal channel. *J. Fluid Mech.* **12**, 241.

HERRING, J. R. & KRAICHNAN, R. H. 1971 Comparison of some approximations for isotropic turbulence. *Statistical Models and Turbulence. Lecture Notes in Phys.* vol. 12, p. 148. Springer.

HERRING, J. R., ORSZAG, S. A., KRAICHNAN, R. H. & FOX, D. G. 1974 Decay of two-dimensional homogeneous turbulence. *J. Fluid Mech.* **66**, 417.

KRAICHNAN, R. H. 1965 Langrangian history closure for turbulence. *Phys. Fluids* **8**, 575.

KRAICHNAN, R. H. 1966 Isotropic turbulence and inertial range structure. *Phys. Fluids* **9**, 1728.

KRAICHNAN, R. H. 1968 Small scale structure of a scalar field convected by turbulence. *Phys. Fluids* **11**, 945.

KRAICHNAN, R. H. 1974 Convection of a passive scalar by a quasi-uniform random straining field. *J. Fluid Mech.* **64**, 737.

KRAICHNAN, R. H. 1977 Eulerian and Lagrangian renormalization in turbulent theory. *J. Fluid Mech.* **83**, 349.

KRAICHNAN, R. H. & HERRING, J. R. 1978 A strain-based Lagrangian-history turbulence theory. *J. Fluid Mech.* **88**, 355.

LESLIE, D. C. 1973 *Advances in the Theory of Turbulence.* Oxford: Clarendon Press.

ORSZAG, S. A. & PATTERSON, G. S. 1972 Numerical simulations of three-dimensional homogeneous isotropic turbulence. *Phys. Rev. Lett.* **28**, 76.